Novel conductance step in carbon nanotube with wing-like zigzag graphene nanoribbons*

Hong Liu(刘红)†

Physics Department, Nanjing Normal University, Nanjing 210023, *China*

(Received 8 May 2017; revised manuscript received 9 August 2017; published online 30 September 2017)

Connecting one armchair carbon nanotube (CNT) to several zigzag graphene nanoribbons (ZGNRs) we find that the topologically-protected edge states of ZGNRs and the massless Dirac particle inherited from CNT still hold from the analysis of the band structure and the edge state. Furthermore, the lowest conductance step at the valley bottom increases proportionally with increasing the number of ZGNR wings. A novel conductance step of a peak occurs in the valley, which is two steps higher than the lowest step at the valley bottom. In addition, with increasing the number of ZGNR wings the width of the novel conductance step becomes narrow.

Keywords: carbon nanotube, Dirac point, edge state, quantum conductance

PACS: 61.46.Np, 61.48.Gh, 73.63.–b, 73.63.Fg **DOI:** 10.1088/1674-1056/26/11/116101

1. Introduction

Since the discovery of carbon nanotubes (CNTs)[1] and the groundbreaking experiments regarding the monolayer graphene,[2] the low-dimensional carbon nano-material has been considered a promising material for future electronics. Extensive experimental and theoretical researches have been devoted to the studying of their various novel physical properties. The subsequent experimental measurement on graphene layers motivates the investigation on the spin quantum transport in graphene.[3,4] Recently, topological surface states (edge states) in condensed matter have received a lot of attention; specially zigzag-edged graphene nanoribbons (ZGNRs) have recently received significant attention due to their unique spin-related electronic structures and the topologically-protected edge states.[5–11] One proposed that the quantum spin Hall effect (QSHE)[12–15] can occur in the topological insulators (TIs) without applying any magnetic field.[16–22] Nowadays, many experimental and theoretical studies focus on looking for new two-dimensional layered materials in order to obtain new two-dimensional TIs having large bulk energy gaps for QSHE in practice. Recently many new two-dimensional TIs have been found such as HgTe/CdTe,[16] InAs/GaSb,[17] and Cd_3As_2[18] quantum-well structures, Bi_2TeI,[19] the bismuth (111) bilayer,[20] and the simple binary compounds $ZrTe_5$ and $HfTe_5$.[21,22] However, by using the known two-dimensional TIs, the assembled quasi-one-dimensional materials have been studied little, especially using two-dimensional graphene. In 2015, Weng *et al.* proposed three-dimensional graphene networks with negative curvature having topologically nontrivial node lines in bulk based on the first-principle calculations.[23] Obviously, the assembled carbon nanomaterials (ACNMs) can help us develop many possible ways to construct new artificial materials or devices with many more expected function effects.

These ACNMs have stable geometrical structures and can be produced artificially due to the various bond configurations of a carbon atom connecting to its neighbor atoms. In the present work, we try to assemble armchair CNTs together with ZGNR slices as a new type of quasi-one-dimensional carbon nanomaterial. We can optimize it by using the empirical potential and the first-principle calculations. We think that these ACNMs have not only the merit characters inherited from both CNTs and graphene, but also some novel effects due to the existence of the sp^3 hybrid bonds connecting the CNT with the ZGNRs.

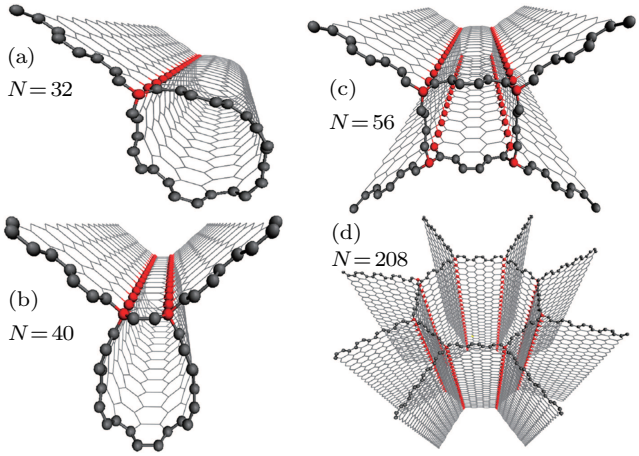


Fig. 1. (color online) Structures of ZW-CNTs based on the tubes (6, 6) and (20, 20), i.e., (a) ZW_1-(6, 6), (b) ZW_2-(6, 6), (c) ZW_4-(6, 6), and (d) ZW_8-(20, 20). The integer N refers to the number of carbon atoms in the primitive cell. For comparison, the red balls show these atoms bonding to four nearest-neighbor atoms by the sp^3 hybrid orbits.

*Project supported by the National Natural Science Foundation of China (Grant No. 10947004) and the Government Scholarship for Overseas Studies of Jiangsu Province, China.

†Corresponding author. E-mail: liuhong3@njnu.edu.cn

© 2017 Chinese Physical Society and IOP Publishing Ltd

As is well known, the ZGNRs have the topologically-protected edge states, and an armchair tube has two Dirac points, so we are interested in using ZGNR and one armchair tube as the elements to build up ACNMs, called CNT with wing-like ZGNR slices (ZW-CNT). In Fig. 1 we show the geometrical structures of the ZW_1-(6, 6), ZW_2-(6,6), ZW_4-(6,6), and ZW_8-(20, 20), respectively, in which the subscript integer refers to the number of ZGNR slices. We find that near the Fermi energy the electronic structure of ZW-CNT is independent of the connected place of ZGNR slices with the tube. In the present work, we take the ZW_n-(6,6) for example to investigate the electronic structure and the transport properties.

2. Electronic structure and quantum conductance

Within the π-electron tight-binding method only considering the nearest neighbors, the band structures of various ZW_n-CNT are shown in Fig. 2. In the calculation the hopping parameter is $t_{ij} = t_0 = -2.75$ eV between two nearest neighbor sites i and j. Because the model neglects the influences of bond length and the angle between two bonds on the hopping parameter, the differences in band structure are caused by the bond configuration in various ZW-CNTs. The band structures of the corresponding (6, 6) tube and pure ZGNR are also shown in Figs. 2(a) and 2(b) for comparison. In addition, although the Hamiltonian only considers one single π-electron, we think that it can still provide the basic characteristics of the electronic structure of the system. The total number of electrons filling in the bands is not equal to the total number of carbon atoms in the system, because the four electrons of the atoms at the connection sites are used to form the four sp^3 hybrid bonds.

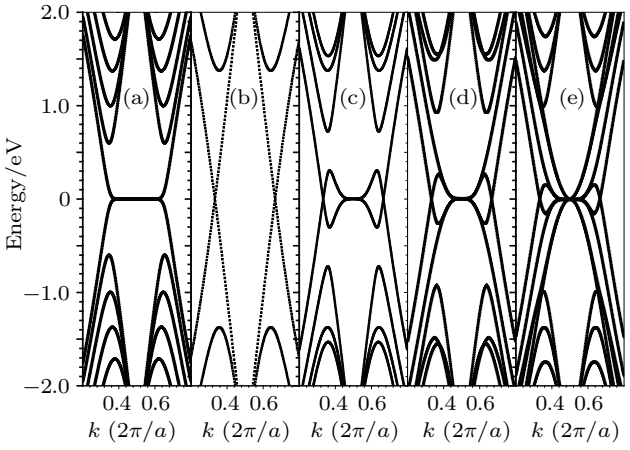


Fig. 2. Band structures of various ZW-(6, 6), i.e., (a) ZGNR ($N = 40$), (b) CNT (6,6), (c) ZW_1-(6,6), (d) ZW_2-(6,6), and (e) ZW_4-(6,6). Tube (6,6) and ZGNR ($N = 40$) given here are for comparison.

Naturally, in the energy region away from the zero energy point, the band structure of ZW_2-(6,6) is similar to that of the pure ZGNR under the condition of the same size ($N = 40$). However, some obvious differences are found in the energy region of interest, near the zero energy. No matter how many wing-like ZGNR slices are connected to the tube (6, 6), the two Dirac points at $\pm 1/3$ inherited from armchair tube (6, 6) still hold. Furthermore, between the two wave vector points $-1/3$ and 1/3, the bands through the Dirac points change direction and go back to zero energy, and the states become edge states, which are shown in Fig. 3 and are discussed below.

Another remarkable feature is that the number of bands drifting into the zero energy increases proportionally with the number of wings increasing.

Considering no spin degree, at the zero energy the numbers of bands are 2, 4, and 8 for ZW_1-(6, 6), ZW_2-(6, 6), and ZW_4-(6, 6), respectively. Taking the ZW_2-(6, 6) for example, in order to illustrate the edge-distribution characteristics of the states in these four bands drifting to the zero energy, in Figs. 3(a)–3(e) we plot the spatially occupied probabilities of the four states in these four bands. From Fig. 3, at the Dirac points $-1/3$ and 1/3 none of the four states is an edge state, but the states of k wave vectors between about 0.4 and 0.6 are all edge states. Especially, at the wave vector $k = 0.5$ the probability of the states reaches 100% at the edge sites 13 and 33, which are the outside edge sites of two ZGNR wings. Obviously, there are two electrons fully distributed at these two outside edge sites, which are shown by the big red balls in Fig. 3(f). It shows that the corresponding two bands originate from the pure ZGNR.

On the opposite-direction edge side of the ZGNR slice, that is to say, at the connection place, the probability distribution is different from that in the case of the pure ZGNR. At the sites 9, 20, 29, and 40, denoted by the relatively small red balls in Fig. 3(f), respectively, the occupied probability is the same value of 50% at $k = 0.5$. At the connection place the four sites 9, 20, 29, and 40 averagely share the two electrons. Obviously, it shows that the two states in the two bands through the Dirac points are the edge states at $k = 0.5$.

By use of the Landauer formula and Green's function method[24–28] the quantum conductance through a region of interacting electrons can be calculated and is shown in Fig. 4. By comparing the two curves of ZW_2-(6,6) and the pure ZGNR ($N = 40$), in the high energy region the quantum conductance steps on ZW_2-(6, 6) on the blue dotted line are similar to those on the black dotted line for the pure ZGNR.

Specially, in the energy region from -1 eV to 1 eV, of interest, there is one novel higher quantum conductance step at the lowest valley for any curve of ZW_n-(6, 6). In the present theoretical model no matter how large the sizes of ZGNR and

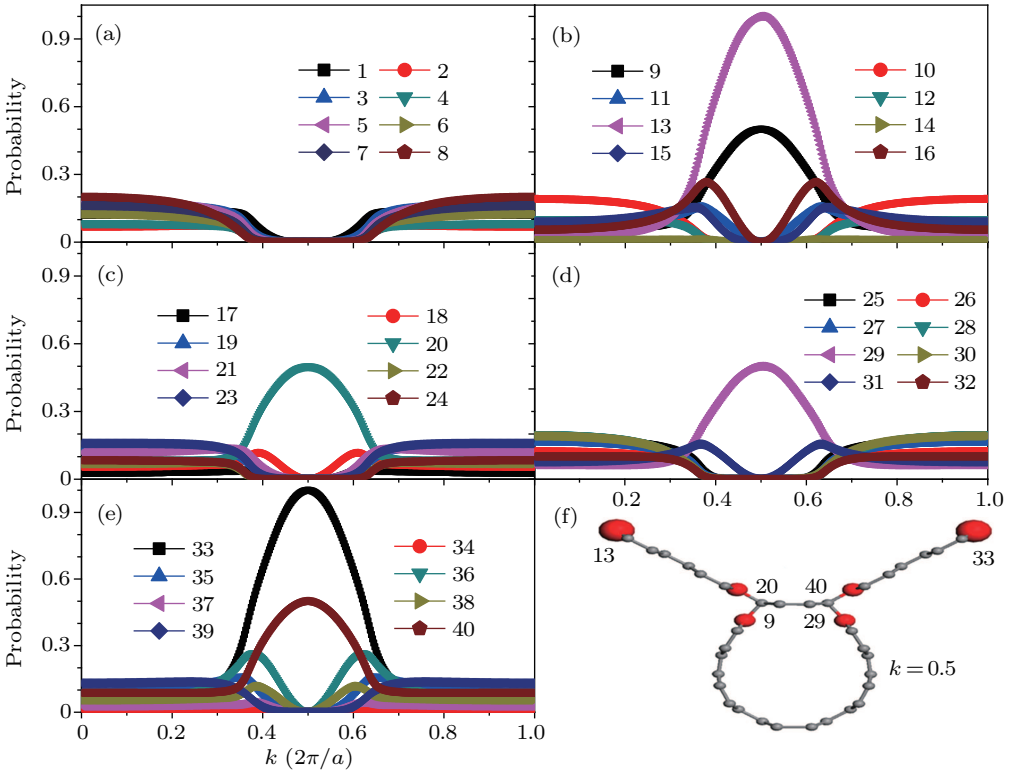


Fig. 3. (color online) Occupied probabilities at sites of states in the four bands drifting into the zero energy in ZW_2-(6, 6) with $N = 40$. The integers refer to the site indices. (a) At 1-8 sites, (b) at 9-16 sites, (c) at 17-24 sites, (d) at 25-32 sites, and (e) at 33-40 sites. (f) In one premitive cell two edge sites 13 and 33 are denoted by big red balls expressing the probability 100%, and the four sites 9, 20, 29, and 40 are denoted by small red balls expressing 50%.

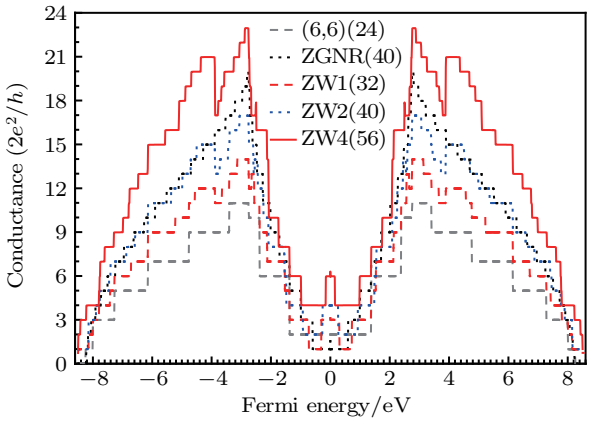


Fig. 4. (color online) Quantum conductances of various ZW_n-(6, 6) ($n = 1, 2, 4$). The integer in brackets refers to the number of atoms in the primitive cell. The quantum conductances for the tube (6, 6) and the ZGNR are also shown for comparison.

the armchair tube are, their lowest conductance steps are always 1 and 2, respectively. However, the lowest conductance steps are 1, 2, and 4 for ZW_1-(6,6), ZW_2-(6,6), and ZW_4-(6,6), respectively, showing that it is not the summation of the lowest steps of CNT and ZGNR slices. That is to say, the lowest conductance step of ZW_n-CNTs is n, which is the number of ZGNR wings.

Remarkably, at the valley bottom there are novel higher conductance steps 3, 4, and 6 for ZW_1-(6,6), ZW_2-(6,6), and ZW_4-(6,6), respectively, which is two steps higher than the corresponding lowest conductance step. Obviously, this increase of two channels for these novel conductance steps originates from the armchair tube. Furthermore, with increasing the number of ZGNR wings the width of the novel conductance step becomes narrower in Fig. 4. It shows that in the narrow energy region around the zero energy point the conductance step is the summation of the lowest steps of CNT and ZGNR slices. From the band structures in Fig. 2 the two bands through the Dirac points change direction to the zero energy. The energies at the turning points of these two bands determine the width of this novel conductance step. According to this result, for ZW_8-(20, 20) in Fig. 1(d) the lowest conductance step can reach 8, and the novel higher conductance step at the valley bottom is 10, which is 10 times higher than the lowest step of one pure ZGNR. It provides a way to build the carbon nanomaterials having much higher conductance in the lower energy region.

3. Conclusions

In our study, for the assembled ZW-CNTs two Dirac points still hold and the topologically-protected edge states of ZGNRs exist. We find that the lowest conductance step in the valley is attributed to the edge states of all connected ZGNR slices. Furthermore, because the bands through the Dirac points change direction to the zero energy, and the states become edge states at $k = 0.5$, there are two channels increased that contribute two conductance steps higher than the lowest

step of the valley bottom. Finally, with increasing the number of wings, the width of the novel higher conductance step at the valley bottom becomes narrow, the number of edge bands increases, and the corresponding lowest quantum conductance step increases proportionally.

Obviously, for this assembled quasi-one-dimensional ZW_n-CNT the conductance in the lower energy region is higher than that for the single CNT or a pure ZGNR. Specially, the existence of the novel higher conductance step at the zero energy can help us to design a more precisely-controlled nanoswitch. Furthermore, due to there being much more atoms in the primitive cell and lower symmetry than those in CNT or ZGNR, it has super strong dipole matrix elements along the axis direction. Naturally, the strong nonlinear optical susceptibility and novel optical effect can be imaged for the incident light polarized along the axis direction. Therefore, in practical applications, we believe that this assembled method provides a way to build various quasi-one-dimensional or quasi-three-dimensional all-carbon nanomaterials for more precisely-controlled nanodevices working in the lower energy region, such as sensitive optoelectronic nanoswitches, thermoelectronics, supercapacitors, hydrgon storage, absorbents, and strong nonlinear optical devices. We will carry out detailed research in the future in order to give a new in-depth insight into the characteristics of edge states and the various properties in this type of ACNM.

Acknowledgment

The author is particularly grateful to her colleague Prof. Guiqin Huang for helping her to revise the text in English and the initial discussion on the optimization of ZW-CNT from the first principle method.

References

[1] Iijima S 1991 *Nature* **354** 56
[2] Novoselov K S, Geim A K, Morozov S V, Jiang D, Katsnelson M I, Grigorieva I V, Dubonos S V and Firov A A 2005 *Nature* **438** 197
[3] Tombros N, Jozsa C, Popinciuc M, Jonkman H T and Van Wees B J 2007 *Nature* **448** 571
[4] Williams J R, DiCarlo L and Marcus C M 2007 *Science* **317** 638
[5] Ezawa M 2006 *Phys. Rev. B* **73** 045432
[6] Fujita M, Wakabayashi K, Akada K and Kusakabe K 1996 *J. Phys. Soc. Jpn.* **65** 1920
[7] Nakada K, Fujita M, Dresselhaus G and Dresselhaus M S 1996 *Phys. Rev. B* **54** 17954
[8] Yang L, Cohen M L and Louie S G 2008 *Phys. Rev. Lett.* **101** 186401
[9] Wakayabashi K, Fujita M, Ajiki H and Sigrist M 1999 *Phys. Rev. B* **59** 8271
[10] Wang Y, Yang S and Niu Q 2009 *Phys. Rev. Lett.* **102** 096801
[11] Liu H, Hu B and Liu N 2016 *Phys. Lett. A* **380** 3738
[12] Bernevig B A, Hughes T L and Zhang S C 2006 *Science* **314** 1757
[13] Yang Y, Xu Z, Sheng L, Wang B G, Xing D Y and Sheng D N 2011 *Phys. Rev. Lett.* **107** 066602
[14] Li H, Sheng L and Xing D Y 2012 *Phys. Rev. Lett.* **108** 196806
[15] Li S 2014 *Progress in Physics* **34** 1
[16] König M, Wiedmann S, Brüne C, Roth A, Buhmann H, Molenkamp L W, Qi X L and Zhang S C 2007 *Science* **318** 766
[17] Knez I, Du R R and Sullivan G 2011 *Phys. Rev. Lett.* **107** 136603
[18] Wang Z J, Weng H M, Wu Q S, Dai X and Fang Z 2013 *Phys. Rev. B* **88** 125427
[19] Tang P, Yan B, Cao W, Wu S C, Felser C and Duan W 2014 *Phys. Rev. B* **89** 041409(R)
[20] Murakami S 2006 *Phys. Rev. Lett.* **97** 236805
[21] Weng H M, Dai X and Fang Z 2014 *Phys. Rev. X* **4** 011002
[22] Wu R, Ma J Z, Nie S M, Zhao L X, Huang X, Yin J X, Fu B B, Richard P, Chen G F, Fang Z, Dai X, Weng H M, Qian T, Ding H and Pan S H 2016 *Phys. Rev. X* **6** 021017
[23] Weng H M, Liang Y Y, Xu Q N, Yu R, Fang Z, Dai X and Kawazoe Y 2015 *Phys. Rev. B* **92** 045108
[24] Kubo R 1957 *J. Phys. Soc. Jpn.* **12** 570
[25] Nardelli M B 1999 *Phys. Rev. B* **60** 7828
[26] Ferreira M S, Dargam T G, Muniz R B and Latge A 2000 *Phys. Rev. B* **62** 16040
[27] Ferreira M S, Dargam T G, Muniz R B and Latge A 2001 *Phys. Rev. B* **63** 245111
[28] Nardelli M B and Bernholc J 1999 *Phys. Rev. B* **60** 16338